Inhomogeneous Thermal Changes in Copper During Plastic Elongation

GERALD L. MOSS AND ROBERT B. POND, SR.

The radiant energy emitted from electrolytic tough pitch copper during plastic tensile elongation was recorded with a photoconductive detection system sensitive to wavelengths from 2 to 30 μm. Radiation measurements were made while Cu samples were deformed at strain rates from 0.56 to 172 s^{-1}. Abrupt changes in emission were correlated with the intermittent plastic action of Lüders bands. It is emphasized that the measurements were of the differences in radiation emitted by nearby points on a sample. The differences in the emitted radiation were due to the inhomogeneous nature of the deformation. A new calibration technique is described that accounts for the optical effects of changes in surface topography and the thermal radiating characteristics of a metal that arise during plastic deformation. This calibration technique was used to associate temperature differences with the radiation measurements and the localized nature of the plasticity. Temperature differences were observed at low average strains that were large enough to imply crack nucleation. Changes in the inhomogeneous temperature-strain data occur at the critical strains that have been reported for many metals. This correlation is very clear at the critical strains of 1.5, 7.5 and 16.4 pct. Whether or not there are real changes at the other critical strains is more speculative.

THERE have been numerous investigations of thermal changes during the plastic deformation of metals, but these have almost invariably dealt with the average temperature change. The accompanying analyses have, therefore, been primarily designed to relate the mechanical work done with the resultant heating and to make an energy balance. However, there is often as much or more interest in the localized thermal changes that develop as there is in average temperature changes. The interest in the localized changes is practically, as well as academically, motivated since physical properties during deformation depend on the thermal state, rather than on the average temperature, of the deforming material.

There have been a limited number of measurements of temperature changes in plastic zones. Most of these observations have been made on samples subjected to extensive shear deformation similar to those found in the machining process. In these situations, the strain occurs within the sample, and there are often obstructions that prevent thermal measurements as deformation occurs. In spite of these difficulties, Erdmann and Jahoda[1] developed an ingenious method for investigating incremental thermal signals developed within tensile specimens. With information gained from thermal sensors on opposite ends of the specimen, they were able to determine the location of the plastic zone in the sample in addition to the shape of the thermal pulse. Uncertainty in the details of the plastic zone, such as its width and orientation, precluded its accurate temperature determination. Nadai and Manjoine[2] reported the measurement of a localized temperature change that is particularly relevant to this paper. In their experiment, they measured a maximum temperature change of 43°C in the neck of an iron sample elongated to fracture. Unfortunately, only one measurement was reported, and apparently no attempt was made to pursue the study. While the investigations referenced above may not have furnished the complete details of localized heating required for all purposes, they very clearly indicate that there can be substantial differences in the localized and average heating, even during tensile elongation.

Here, the purpose has been to develop an infrared (IR) measuring technique that can be used to monitor the development of thermal changes at operative plastic zones. The technique depends on recording the change in infrared radiation emitted by a sample as it deforms and relating the recorded information to the changes in the thermal state of the sample. This is not the first time that this technique has been used to investigate thermal changes during plastic deformation. There was one paper published before, and several have been published since, this work began.[3-8] However, in each case, the emphasis was on the average change in thermal state, while here, the report is of, what is believed to be, the first application of the technique to the direct measurement of localized thermal changes. In general, previous studies of heating during deformation that have been made with the infrared technique have met with limited success. Hence, part of this investigation has necessarily dealt with data interpretation. Since these considerations are new, they are presented in moderate detail in an Appendix.

RADIATION DETECTION SYSTEM

There are at least two good reasons for resorting to an infrared radiation detection technique for investigating thermal changes during plastic deformation. First, it is a noncontact measuring technique, and secondly, most of the thermal radiation emitted by a

GERALD L. MOSS is Acting Chief, Solid Mechanics Branch, Ballistic Research Laboratories, Aberdeen Proving Ground, Md. 21005. ROBERT B. POND, SR., is Professor and Chairman, Department of Mechanics and Materials Science, The Johns Hopkins University, Baltimore, Md. 21218. This paper is based on a portion of a thesis submitted by Gerald L. Moss in partial fulfillment of the requirements of the degree of Doctor of Philosophy at The Johns Hopkins University.

Manuscript submitted November 5, 1973.

solid is in the infrared. For example, a black body radiates at room temperature with Planck's spectrum and with a maximum intensity at a wavelength of approximately 10 μm. The radiation from a metal is essentially the same except as modified by the spectral emissivity of the metal.

In preliminary considerations, it was expected that various thermal studies would eventually be pursued. The range of experimentation envisioned specified that the detection system should have a microsecond response, be sensitive to temperature changes of only a few degrees and resolve at least 0.025 cm. It was found that these features were only attainable by using the fullest capabilities of currently available detectors. Consequently, all the detectable energy was recorded in this work to maximize sensitivity, and the changes in surface topography through plastic deformation were taken into special account.

The detection system is shown in Fig. 1. A Cu doped Ge (Ge:Cu) single crystal semiconductor was used to sense the changes in radiation. This detector responds to radiation with wavelengths between 1.8 and 30 μm and is, therefore, sensitive to the radiation that is predominantly emitted at room temperature. A characteristic of Ge:Cu detectors is that they only function at temperatures below 20 K. This accounts for the liquid He dewar positioned over the detector. The pair of mirrors under the detector were relied upon to collect enough radiation to give signals above noise for the other system characteristics that were considered desirable. These included a 5.6×10^{-4} cm^2 field of view and a 3.5×10^4 Hz electrical bandwidth. With these design parameters, there was a minimum detectable black body temperature of 0.11°C. The samples studied were placed at the focal point of the mirror system, and this condition was essentially preserved throughout deformation.

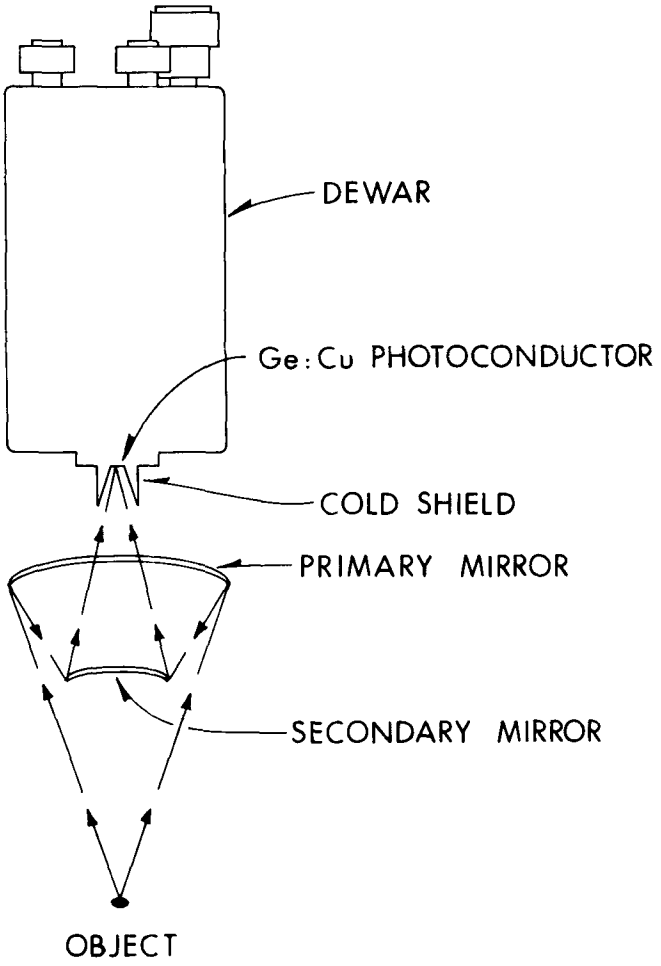

Fig. 1—Infrared detection system.

MEASURED INHOMOGENEOUS THERMAL CHANGES DURING DEFORMATION

Material

Electrolytic tough pitch copper was used throughout this work. The nature of this material is partially documented with the stress strain curve shown in Fig. 2. The surfaces to be observed with the infrared detection system were cleaned within two days of testing by grinding with 600 grit silicon carbide under cool tap water. Once prepared, the samples were dessicated until test time. The surface roughness after grinding was found, by optical comparison with polished surfaces, to be essentially smooth at the detectable wavelengths.

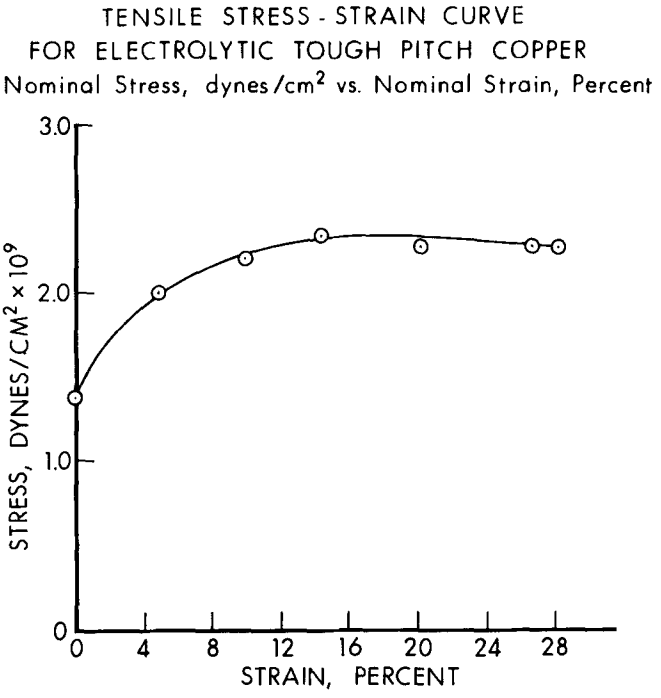

Fig. 2—Deformation curve of electrolytic tough pitch copper used in thermal studies.

Loading Technique

There was practically no prior experimental information to suggest the magnitude of the thermal inhomogeneities to be encountered which made it rather uncertain that there would be any hot enough to detect. Hence, an attempt was made to accentuate them by using a pneumatic loading device. The presumption was that such a loading mechanism would allow plastic instabilities to develop abruptly and, hopefully, result in measurable isolated temperature changes. A

"hard" machine might, alternatively, constrain the rate of development of a plastic instability so that potential thermal gradients would be nearly wiped out. Also, a hard machine could significantly reduce the extent of deformation per instability. The loading system used (Allied Research Associates, Model P-18) had dual pistons that were driven with compressed air. Low deformation rates were obtained by gradually pressurizing the pistons through a "system-seal" valve. High strain rates, 59 to 172 s^{-1}, were obtained by loading the pistons which transmitted the load to a steel load bar that was placed between two identical copper samples. When the pressure become large enough to break the steel, the copper samples were deformed to fracture.

All tensile specimens were machined with 6.02 cm between the shoulders of the grips and with a cross section of 0.0559 by 0.508 cm. During deformation, the sample was held between gimbal grips; however, the vertical position of the specimen was mechanically fixed so the observed surface of the specimen remained within ±0.0004 cm of the focal point of the detection system. This is a small distance compared with the optical depth of field and means the constraint effectively avoided any problems from general surface tilting or displacement until fracture.

The average deformation of the copper was monitored with an optical displacement gage (Model 1013 with 0.127 cm sector width and gate, Allied Research Associates, Inc.).

Radiation Measurements

Before each test, the IR detection system was focused on the copper sample and oriented with signals obtained by chopping the radiation from the copper specimen. Orientation and focusing adjustments were invariably made so the recorded signals were a maximum and had a shape with a double overshoot which was a characteristic due to the amplifier. During deformation, the signals from the infrared system and the displacement gage were simultaneously recorded on a dual beam Type 551 Tektronix oscilloscope with Type Z Plug-in units. This recording method automatically synchronized the deformation and thermal records. On some occasions the thermal signals were also recorded on another oscilloscope, Tektronix 535A with a 53/54 L Plug-in unit.

It was suspected that the voltage signals due to the thermal inhomogeneities of the low strain-rate tests might occur with frequencies below the bandwidth of the recording equipment. To insure that these signals would be recorded faithfully, the observed radiation was chopped at 10^3 Hz with a tuning fork (American Time Products, Model 40C). It was found that the temperature gradients were such that it was unnecessary to chop the radiation during the high strain-rate tests.

Results

Radiation and displacement records obtained while copper samples were elongated at different rates are shown in Figs. 3 through 10. A prominent feature of the radiation records is that there are very rapid voltage changes compared with the total deformation time. These are superimposed on a more gradual voltage increase that continued throughout the deformation. This is evident in each of these records except the one shown in Fig. 5, which is a record of a test in which the deformation rate was so slow that the gradual thermal change was substantially below the minimum frequency response of the amplifier. Hence, no voltage change was recorded to indicate the gradual temperature change. The same would have been true of the changes shown in Fig. 3 except

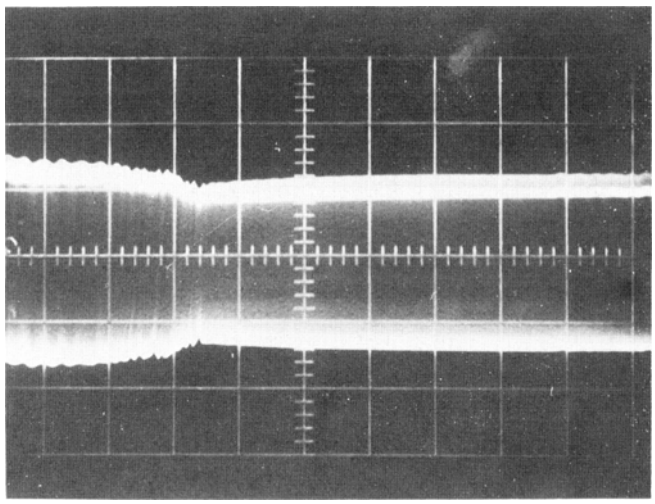

Fig. 3—Voltage changes recorded with the infrared radiation detection system during deformation. Chopped radiation. Vertical scale, 1 volt/cm; horizontal scale, 0.5 s/cm. The strain-time data corresponding to this record is shown in Fig. 4. The maximum strain rate was 0.56 s^{-1}. The deformation was stopped after approximately 1.5 s.

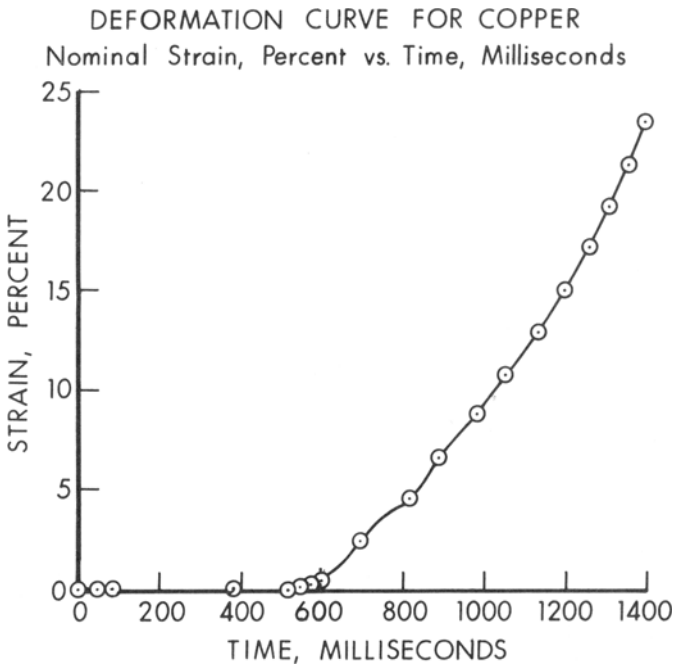

Fig. 4—Deformation data corresponding to the radiation measurements shown in Fig. 3. In this test the sample thickness was 0.166 cm rather than the usual 0.0559 cm. The other dimensions of the sample were the same as in the other tests reported. The load was applied by opening the system seal air valve so the pistons of the loading device filled gradually during the test.

that the chopping technique used in that test revealed the gradual changes. It is emphasized that the deformation rates of all the tests to be reported were such that the gradual underlying voltage changes were below the frequency response of the radiation detection system. Hence, they were never recorded properly even though there was a definite manifestation of their occurrence. On the other hand, the high frequency voltage changes recorded in the higher strain-rate tests were within the bandwidth of the detection system so they were recorded properly.

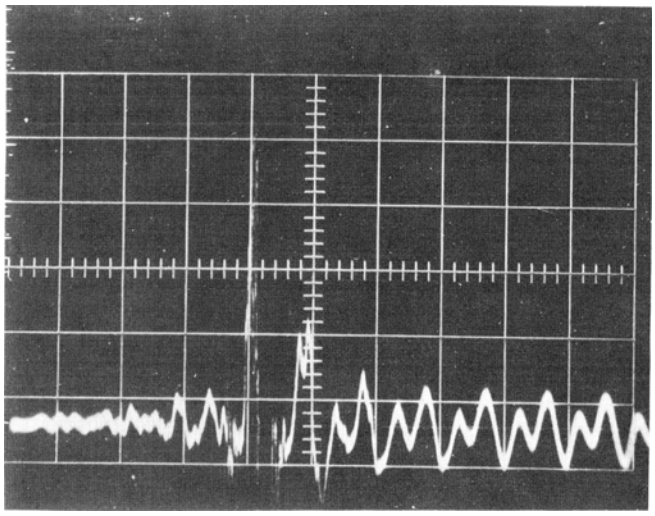

Fig. 5—Voltage changes recorded with the infrared radiation detection system during deformation. Vertical scale, 0.2 volts/cm; horizontal scale, 20 ms/cm. The strain-time data corresponding to this record is shown in Fig. 6. The maximum strain rate was 9.3 s^{-1}. Fracture occurred after approximately 69 ms.

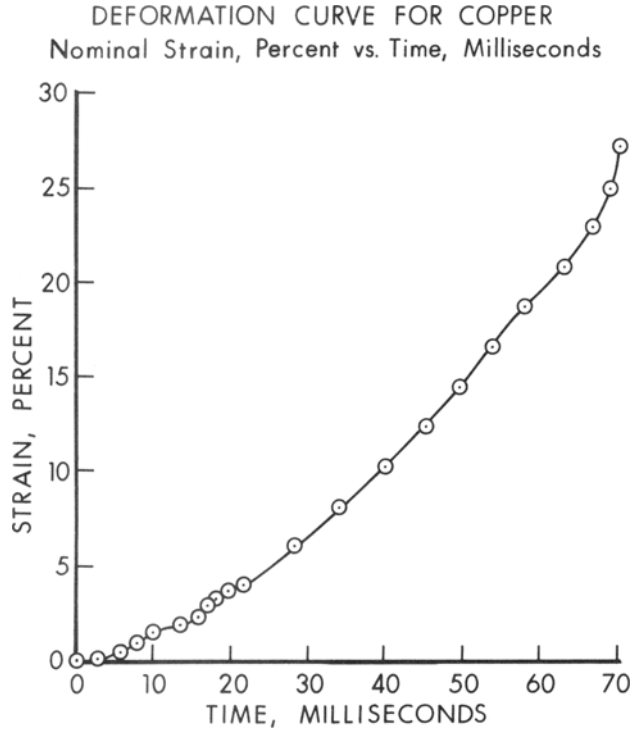

Fig. 6—Deformation data corresponding to the radiation measurements shown in Fig. 5. The load was applied by opening the system seal air valve so the pistons of the loading device filled with air during deformation.

Interpretation of Results

The conversion of the radiation measurements to information about thermal change was made by taking into account previously ignored factors. The technique employed is new as are some features of the deformation that were revealed by the spatial differences in detectable radiation. A description of the method of treating the data, calibration procedures, and the features of the deformation that were revealed by the measurements are given in the Appendix. This allows a concise presentation of the thermal results, but it is not as straightforward as if the details of the plastic deformation and calibration were given first. To avoid confusion, a brief description of the inhomogeneous nature of the deformation is given next.

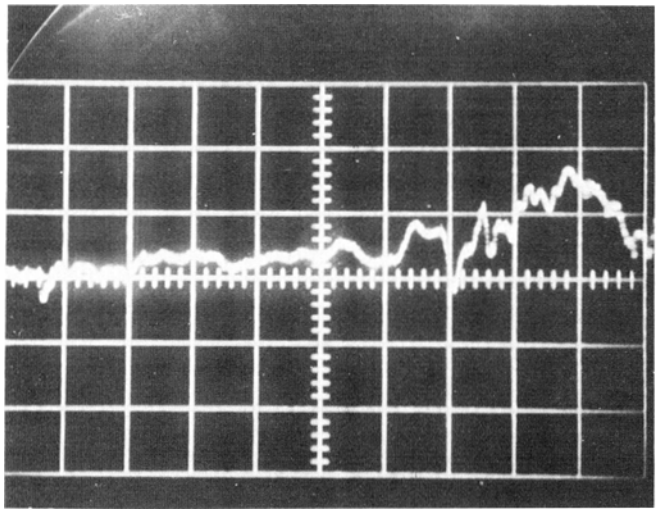

Fig. 7—Voltage changes recorded with the infrared radiation detection system during deformation. Vertical scale, 0.62 volts/cm; horizontal scale, 1 ms/cm. The strain-time data corresponding to this record is shown in Fig. 8. The maximum strain rate was 59 s^{-1}. Fracture occurred after approximately 8.8 ms.

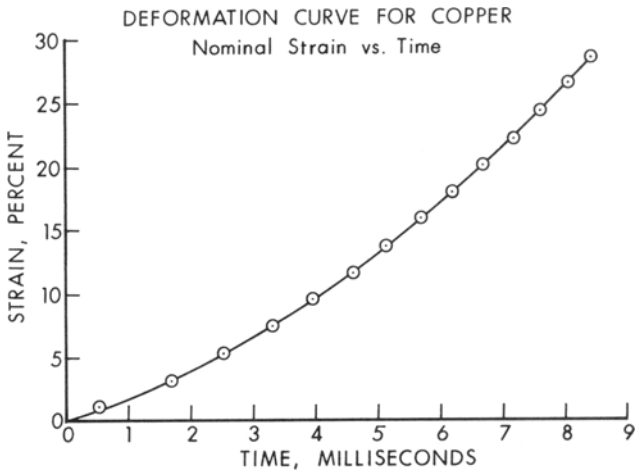

Fig. 8—Deformation data corresponding to the radiation measurements shown in Fig. 7. A steel load bar was used in the stress application.

The radiation measurements revealed that Lüders bands developed in the Cu investigated (see Appendix), and it was found that the temperature differences from band to band could be investigated. The expression "Lüders band" is often used to refer to the bands of permanent deformation that develop in steel at yield on planes that are approximately parallel with the planes of maximum shear stress. There is a wider application of the expression, however, as used by Phillips et al.[9] to describe diffuse bands such as those that form in Al-Mg alloys throughout the course of plastic deformation. Now that the occurrence of discontinuous repeated yielding is well established (see Appendix), the differences in the two cases might be viewed as more in degree than kind. While the bands that formed in the Cu may have special characteristics, they will be referred to as Lüders bands. This should lead to no confusion since their special properties are described in the Appendix. Briefly, the bands formed at yield such that their domain was essentially established, their width along the tensile axis was approximately 0.02 cm, and plastic deformation occurred throughout deformation by the localized discontinuous repetitive action of these same bands.

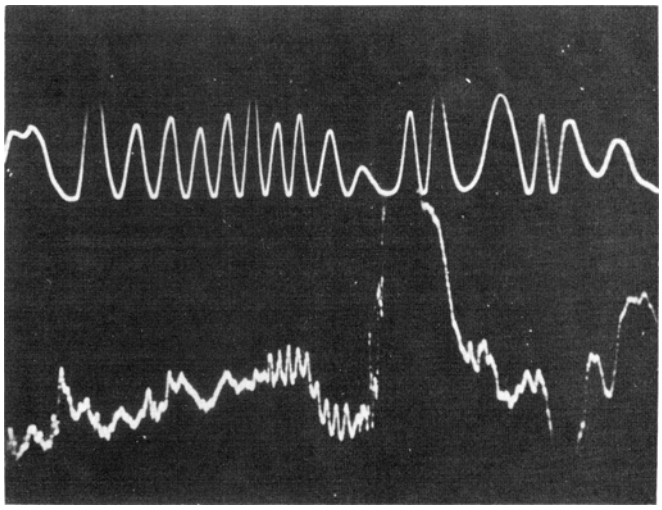

Fig. 9—Voltage changes recorded with the infrared radiation detection system during deformation, lower trace. Vertical scale, 0.5 volts/cm; horizontal scale, 1 ms/cm. The upper trace is the record from the displacement-time gage. The strain-time data corresponding to this record (Sample 1) is shown in Fig. 10. The load was applied with the steel load-bar technique. The maximum strain rate was 122 s^{-1}. Fracture occurred after approximately 4.1 ms.

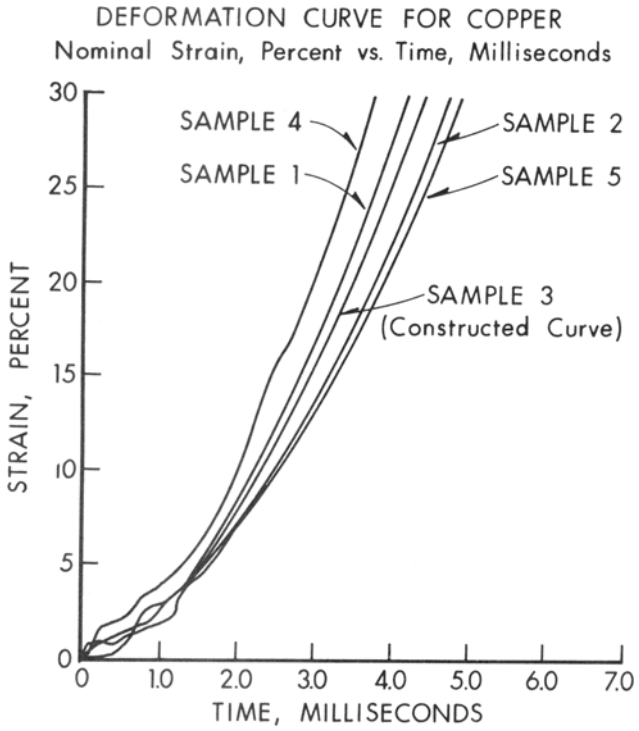

Fig. 10—Deformation data corresponding to the high strain-rate tests. Steel load bars were used in the stress application to get the high strain-rates.

In general, the width of the high frequency voltage changes are similar to those from surface scans of previously deformed and thermally equilibrated copper samples (see Appendix). This is taken to mean that the high frequency voltage changes measured during deformation stemmed from the development of Lüders bands since these were related to the voltage increments on the records of the post-test surface scans. An additional feature evolved at low strain levels during slow strain-rate deformation (see Fig. 3). There, the high frequency voltage changes are similar to sinusoidal oscillations rather than abrupt incremental changes. Comparison of Figs. 3 and 4 clearly verifies that the voltage oscillations in Fig. 3 were not related to surging of the air in the pistons of the loading device. Instead, the oscillatory behavior was a consequence of heat conduction that became a major effect in that test because the deformation was very slow (0.56 s^{-1} maximum). At the strain rate of 122 s^{-1} (see Fig. 9), there were, however, voltage changes that occurred in the same time it would have taken a sharp boundary on the sample to have crossed the field of view of the radiation detection system. This is substantial enough evidence that nearly adiabatic heating was observed.

The abrupt voltage changes observed in these tests appeared to be the type that could be investigated as adiabatic thermal changes within Lüders bands (see Appendix). This is even true of some of the voltage increments on the records obtained at the slower strain rates since the voltage increments were very abrupt. Several more tests were run at the higher strain rates so that this contention could be investigated further. The related strain-time data is given in Fig. 10. In all of the radiation records that have been reproduced, the time increases from left to right. Also, when it was appropriate, the approximate time to fracture was listed below each figure. After fracture, the samples were free to move with respect to the optical detection system so the voltage changes on the records after fracture should be disregarded.

To find the temperature differences related to the development of Lüders bands it was necessary to read the pertinent voltage changes from the records. The signal obtained with chopping (Fig. 3) was not used because there were substantial conduction effects evident in that record. From the other records, each peak-to-peak voltage change was measured with respect to the position of the trace just before the change occurred. This automatically removed the average temperature change of the overall sample that developed throughout

the deformation, and it left a voltage increment related to the difference in temperature of a Lüders band and the adjacent material. The peak-to-peak voltage measurement included the noise level which was subtracted to get the voltage change due to real effects. Both increasing and decreasing voltage increments were read.

Even though the voltage changes caused by inhomogeneous deformation had been isolated at this point, there were still several factors that contributed to the raw data. Included were the changes in the intrinsic emission from the sample, the reflected radiation from the surroundings, the cavity effect (see Appendix) and the Lambert radiating characteristics of the surface. It is shown in the Appendix that these factors combine to give a voltage increment ΔV_p that must be subtracted from the measured voltage increment ΔV_i. Then, the temperature increment associated with a measured voltage increment, ΔV_i, due to the difference in the plastic development of contiguous material is given by

$$\Delta T = \frac{\Delta V_i - \Delta V_p}{(\partial V/\partial T)_e} \quad [1]$$

Both ΔV_p and $(\partial V/\partial T)_e$ were taken as the values applicable at the average strain of the sample at which ΔV_i was measured. These values were determined by the method described in the Appendix.

It is noted that the difference in ΔV_i for a particular deformation and ΔV_p for an average change cannot be used to find the exact temperature change associated with a specific deformation. It makes more sense to take the difference of like quantities so the voltage increments, ΔV_i, were averaged. Presumably, an average difference in ΔV_i and ΔV_p would lead to an average local temperature difference due to inhomogeneous plastic deformation. It is not necessarily undesirable to determine the average result since this may be most representative of general behavior. In any event, the average local temperature difference was determined for all average strains out to fracture.

The higher strain-rate tests (Samples 1 to 5) were intended to be identical so that good average values of ΔV_i could be found, and only data from these tests were used for this purpose. Actually, the loading was different in each of these supposedly identical tests (see Fig. 10). However, the differences in the strain rates obtained are small compared with the gamut of previously investigated strain-rate effects on copper, *i.e.*, 10^{-9} to 10^{4} s^{-1}. Throughout this entire range of strain rates there are only gradual changes in the mechanical behavior of copper so it was assumed that the high strain-rate tests reported were essentially identical.[2,10,11]

In averaging the voltage increments, an attempt was made to include data from a wide enough average strain interval so there would be several data points to average. Simultaneously, an attempt was made to average data from a small enough strain interval so the dependence of the average ΔV_i on strain would not be lost. Specifically, all increments from 0.0 to 0.1 pct strain were averaged at 0.1 pct strain, data from 0.1 to 0.5 percent strain were averaged at 0.3 pct strain and for strains between 0.50 and 0.95 pct, all the increments were averaged that occurred within ±0.05 pct of the nearest tenth percent strain. At strains above 0.95 pct, the increments that occurred within ±1/2 pct of an integral value of strain were averaged.

Finally, the average local temperature differences due to isolated plastic deformation were calculated from the average values of ΔV_i by applying the method described above. These results are plotted in Fig. 11 as a function of the average strain of the sample. They are believed to be the difference in average temperature of Lüders bands and adjacent material. The bands about the points plotted in Fig. 11 indicate the deviation from the mean.

As already indicated, a specific voltage increment measured with the infrared detection system cannot be converted to an exact temperature increment because the corresponding specific value of ΔV_p is unknown. However, some of the observed voltage increments, ΔV_i, were much greater than the average voltage change due to topography, *i.e.*, ΔV_p. It was felt that significant observations would be lost if the large values of ΔV_i were completely neglected or camouflaged through averaging. Hence, the average values of ΔV_p were subtracted from some of the large unaveraged voltage increments and temperature changes were calculated according to Eq. [1]. These results are listed in Table I. To emphasize the magnitude of the voltage increments in question, the maximum values of ΔV_p (see Fig. 13, Appendix) were used to calculate temperature increments. These differences are also listed in Table I. These calculations are not completely defendable, but they do minimize the magnitude of the temperature increments. Still, some of them are very large, although the correct magnitudes are uncertain.

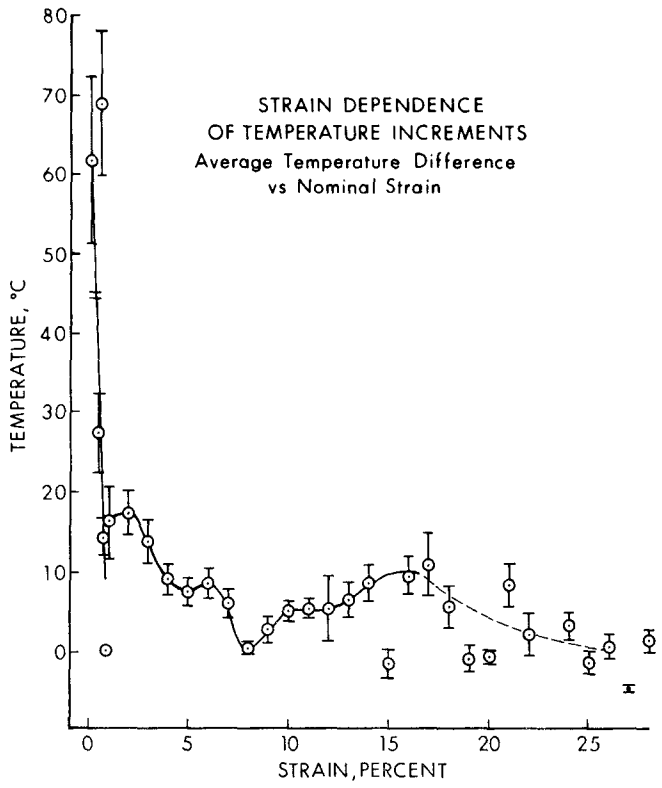

Fig. 11—Average local temperature differences in copper due to inhomogeneous deformation.

Table I. Localized Temperature Differences Measured During Deformation (Data from Figure 7)

Time, s X 10^{-3}	Nominal Strain, Pct	V_i, Volts	V_p (Average), Volts	T, °C	V_p (Maximum), Volts	T, °C
1.97	3.8	0.25	0.026	36.1	0.08	27.4
3.36	7.6	0.08	0.035	6.3	0.14	†
5.2	13.8	0.17	0.046	13.8	0.20	†
5.53	15.2	0.16	0.048	11.9	0.21	†
6.17	17.8	0.36	0.052	30.5	0.22	13.9
6.50	19.3	0.11	0.056	5.1	0.23	†
6.90	20.9	0.55	0.060	44.5	0.23	29.1
7.09	21.8	0.34	0.063	24.7	0.24	8.9
7.34	22.8	0.42	0.066	30.8	0.24	15.7
7.52	23.7	0.46	0.070	33.3	0.25	17.9
7.61	24.1	0.28	0.072	17.6	0.25	2.5
7.90	25.6	0.08	0.078	0.2	0.26	†
7.96	25.8	0.29	0.079	17.2	0.26	2.4
8.13	26.8	0.14	0.084	4.4	0.27	†
8.30	27.7	0.09	0.086	0.3	0.28	†
8.32	27.8	0.06	0.088	†	0.28	†
8.41	28.3	0.16	0.091	5.3	0.29	†
8.56	29.3	0.18	*	–	*	–
8.70	30.2	0.20	*	–	*	–

*Unknown.
†Not tabulated because $|V_i| - |V_p|_{max} < 0$.

Discussion of Results

The copper samples were deformed under ambient conditions, and as such, they were coated with cuprous oxide. Normally, oxides are brittle relative to metals, and it should be expected that the oxide coating on the copper samples broke as they were elongated. While there are many complex processes involved, the major detectable changes are due to 1) the exposure of pure copper as the oxide breaks and 2) the emission of radiant energy from the oxide as its elastic energy is released by the cracking.

The first effect occurs because the oxidation of copper at room temperature is a reasonably slow process. Rhodin has shown that the average thickness of the oxide formed on copper at room temperature is 16Å and that it takes approximately 1/2 h to form.[12] His data suggests that there would have been negligible reoxidation of any pure copper exposed during the high strain-rate tests of this work. If the volume of oxide on the tested samples is assumed to have been constant, and it is noted that the emittance $\epsilon(\Delta\lambda, \Delta\omega, T)$ was 0.04, while the equivalent emittance of pure Cu with no oxide on it is only 0.018,[13] it follows that there was a change in emittance of the observed surface that depended on strain e according to the relation

$$\Delta\epsilon = (\epsilon_{Cu} - \epsilon_{Cu+Cu_2O})e. \quad [2]$$

The emittances given above apply at room temperature and for the wavelength interval and collection angle of the detection system. Since the emittance of the copper tested was greater than the emittance of pure copper, there was a decrease in emittance with strain due to the cracking of the oxide.

If the decrease in emittance is interpreted as causing an error in the thermal measurements, it can be shown that the difference from the reported temperature increments is given by

$$\Delta(\Delta T) = \Delta T(\epsilon_2 - \epsilon_1)/\epsilon_1, \quad [3]$$

where ϵ_1 and ϵ_2 are the emittances before and after the formation of the strain increment.

The percentage error in the reported temperatures due to the cracking-exposure effect can be estimated from the results that have been reported if the error is small. If the error is first assumed to be negligible, the strain of a plastic increment can be calculated from the reported temperature increment by assuming that all the plastic work is converted into heat. From the strain, ϵ_2 is calculated using Eq. [2]. At a nominal strain of 10 pct, the average temperature increment was 5°C. The related incremental longitudinal strain is 4.9 pct, ϵ_2 follows as 0.039 and $\Delta(\Delta T)$ is −0.125°C. Hence, the assumption that the error in the reported temperature increments is negligible is correct, which means the estimate of the error is reasonable. The error from the cracking-exposure effect is, therefore, no more than 2.1 pct.

An upper bound on the error that comes from oxide cracking and the release of its elastic energy is, in principle, readily found by assuming that all the elastic energy is converted into heat. There are, however, practical problems in making the estimate because apparently the modulus and tensile strength of Cu_2O have not been determined. Furthermore, the physical properties of the thin oxide film on copper are not necessarily the same as those of relatively massive samples. Accordingly, the tensile strength and Young's modulus could only be estimated from the known properties of other oxides. However, reasonable values were found to be 9,100 and 8.5×10^6 psi respectively. With the assumption that the oxide is nonplastic, it was found that the maximum temperature change that could occur from the release of elastic energy from the oxide is only 0.012°C which is negligible compared with the thermal changes reported. The actual temperature change must be considerably less because of the energy required for the development of the fracture surfaces. The surface energy is a major factor, and if one considers the situation in which the oxide is loaded to its ultimate strength once, the fracture surface energy required if a crack developed every 10 to 100 microns would be approximately equal to the elastic energy, and there could be only slight heating possible.

The effect of energy emission from the oxide atoms that are actually separated by fracture might be questioned, but the related contribution to the reported measurements is negligible. This is because these localized changes involve electron transitions, and the associated energy emission is typically at higher frequencies than detectable with a Ge:Cu photon counter.

Changes in radiation detected from the surroundings through topographic changes due to oxide breaking were negligible because the oxide thickness is much smaller than the wavelength of the detectible radiation.

There is another temperature change that has been ignored. This is the temperature change first described by Lord Kelvin[14] and usually referred to as the thermoelastic effect. This is given by the equation

$$\Delta T = \frac{T_0 \alpha_l (\Delta\sigma)}{J_\rho C_p}, \quad [4]$$

where T_0 is the initial temperature, α_l is the linear coefficient of thermal expansion, J is the mechanical equivalent of heat, ρ is the density and C_p is the heat capacity. The temperature change is positive in compression and negative in tension. The ultimate tensile strength of the Cu was 2.34×10^9 dynes/cm^2 (see Fig. 2). The corresponding true stress is 2.71×10^9 dynes/cm^2 which, by Eq. [4], suggests the maximum thermoelastic temperature change should have been only -0.41°C.

Since the observed Lüders bands were approximately the same width as the field of view of the detection system, it can be concluded that if the temperature were uniform within a band, it is justifiable to report the temperature differences as in the above. However, during the rise and fall of a voltage change, the signals do not necessarily relate to a specific temperature. The reason for this is that when the boundary of a heated region moves into or out of the field of view, the observation must be of material in several thermal states. Similarly, the results must be clouded because the Lüders bands occurred with a variable thickness some of which were less than the diameter of the field of view.

There is an indication that at times thermal inhomogeneities were observed that were confined to a much smaller region than the width of the Lüders bands. These signals were observed primarily as deformation began. The main reason for suspecting that the signals were not due to Lüders bands is that they did not persist long enough for bands 0.02 cm wide to move out of the field of view once they were formed. For the very fastest crosshead speeds, this would have taken on the order of 0.07 ms, while the duration of these signals was less than this. Instead of persisting, these signals decayed very rapidly to the level of the oscilloscope trace before the disturbance was encountered.

Since these signals were primarily encountered as the load was first applied, one might wonder if they were a consequence of the loading technique. It is reasonable to suspect that stress waves and vibrations might have been generated by the loading technique, and surface tilting from either of these effects would have caused signal changes. It is clear from the experiments of Nadai and Manjoine that at least weak stress waves must have been introduced.[2] Also, noninstantaneous or asymmetric fracture of the steel load bar could have caused the sample to vibrate. Hence, stress waves and vibrations must be acknowledged. It is only the magnitude of their effects on the infrared radiation that is in question. In either event, the signals should have occurred at regular time intervals, damped out regularly with time and been similar in identical tests. None of these features were observed so it is concluded that these voltage spikes were not due to either stress waves or vibrations. This conclusion should be viewed with some caution because the complex grips could have introduced very complicated stress wave interactions. This should, perhaps, be investigated further.

Another possibility is that these abrupt signals may have resulted from extensive slip on a few widely spaced slip bands. The description "widely" is relative to their thickness. The spacing could still have been much less than the thickness of a Lüders band. In fact, the slip bands might have been an underlying feature of an active Lüders band. The acoustic measurements by Fisher and Lally of purported slip bursts in copper indicate that the rapid rise times (less than 0.01 to 0.05 ms) encountered could very well have been due to slip.[15] Detectable signals from slip bands could have resulted, provided the accumulated emission from all the simultaneously observed slip bands occurred as a pulse within the bandwidth of the detection system. If only a small fraction of the surface slipped, as postulated, the average emittance of the material in the field would have remained almost constant. This would be consistent with the observation that there tended to be no substantial permanent voltage change associated with these voltage spikes. Hence, these spikes are of considerable interest since they imply that extensive slip may have occurred with substantial concomitant heating. If this had been the general behavior, the multiple thermal states viewed would have had to have been taken into account, but there was only limited evidence of detectable thermal inhomogeneities on the scale of slip bands. On the other hand, the magnitude of these signals implies substantial heating that might be worth further investigation.

When the voltage increments from a single test were plotted versus strain, the results seemed to bear no particular relationship with strain. However, the average results shown in Fig. 11 vary continuously with strain up to a strain of 15 pct. After approximately 15 pct strain, a few large voltage increments were usually recorded. It is believed that these were a consequence of substantial necking. It is noted that the ultimate tensile strength occurred at a strain somewhere between 14 and 19 pct (See Fig. 2). These large isolated voltage increments undoubtedly caused the scatter in the average temperatures plotted at strains above 15 pct. Hence, no attempt was made to draw a line through all the data points plotted beyond this strain. Instead, a dashed curve was drawn to roughly approximate the general trend of all the data. After observing the average data in Fig. 11, it became clear that the individual increments, ΔV_i, from a single test were also noticeably smaller in the vicinity of 8 pct strain than elsewhere. However, the other features of the curve shown in Fig. 11 were not suggested by the raw data. On the other hand, a comparison of the curve in Fig. 11 with the plastic transition strains of Bell reveals several similarities.[16] The data are compared in Table II where it can be seen that there is one change or another in the thermal data that very closely matches each of the transition strains. Furthermore, a comparison of the thermal increments with the behavior of Portevin-Le Chatelier steps in polycrystalline aluminum, as reported by Sharpe, reveals that both $d(\Delta T)/de$ and $d(\Delta\sigma)/de$ are zero at strains near 5 and 11 pct.[17] Here, $\Delta\sigma$ is the change in stress required to develop a plastic instability (Portevin-Le Chatelier step). Furthermore, the scatter in the magnitude of the strain increments Sharpe reported increased considerably as the strain increased beyond 12 pct. This is consistent with the data shown in Fig. 11 for the temperature increments. The agreement of the dependence of the thermal increments on strain with the transition strains of Bell is taken as strong evidence that the average temperature increments reported are meaningful. In addition, the

Table II. Change in Slope of the Curve of ΔT *vs* Strain

Temperature Increments		Critical Strains*
Nominal Strain, Pct	Condition Observed	(After Bell)
0.8	Minimum	–
1.6	Maximum	1.5
4.8	Minimum†	
6.0	Maximum†	4.2
7.6	Minimum	7.5
10.2-12.0	Plateau	11.5
16.4	Maximum	16.3
26	Minimum	26.6

*The critical strains listed in the table are those given in Reference 16. On February 4, 1972, Bell indicated that the critical strains should be revised to the following: 1.5, 4.1, 7.6, 11.4, 17.1., 25.6.

†If the heating data near these strains is interpreted as a plateau, it would extend from 4.2 to 6.2 pct strain.

agreement with the behavior of Portevin-Le Chatelier steps is further evidence that the thermal inhomogeneities that have been observed are manifestations of plastic deformation within Lüders bands.

While the measured temperature increments depended on strain, there was a large range in the magnitudes of the increments measured at all strains. The average of all those measured was 8.6°C. If it is assumed that 100 pct of the mechanical work went into plasticity and heating, the local plastic work must have been 3.31×10^7 ergs/gm. This corresponds to a longitudinal strain of 14.4 pct. According to the Taylor aggregate theory, the longitudinal true strain, e_t, and the shear strain, γ, are related by

$$\sum_{s=1}^{n} d\gamma_s = 3.06\, \Delta e_t \qquad [5]$$

from which the average shear strain is found to be 44 pct.

The data suggests that temperature differences greater than 18°C may have been observed at nominal strains substantially below those where fracture occurs. If temperature differences of this magnitude did occur, local deformations must have occurred with enough total strain to have caused fracture. This implication was checked by surveying the deformed samples with an optical microscope. These observations revealed many surface cracks. The density of these cracks was greatest after large average strains, but some were obvious well before complete fracture. In general, these crack nuclei occurred at the intersection of Lüders bands at the sample surface. Presumably, complete separation did not occur because the crack nuclei become blunted as they moved out of the zone where the Lüders bands intersected.

CONCLUSIONS

I) The plastic extension of electrolytic tough pitch Cu can proceed with the development of Lüders bands. The number of bands detectable with the radiation detection system employed here increases linearly, but only slightly, with strain. Their prominence also increases with strain suggesting that they tend to continue to function as individual bands throughout deformation to fracture.

II) At strain rates of 100 to 172 s^{-1}, the average temperature differences across the boundaries of Lüders bands depended on the strain, but ranged from 0 to 18°C. The average of all the measured temperature differences was 8.6°C.

III) Temperature differences, implying strains large enough to cause cracks, occur at average strains considerably below the average strain that corresponds with fracture. Furthermore, crack nuclei develop before complete failure, which is in agreement with the thermal measurements. This is presumably possible because the crack nuclei become blunted as they propagate into relatively undeformed material.

APPENDIX

Calibration of Detection System

The simplest calibration, and the one that is most often used, applies when there is a temperature change alone. It is assumed that the voltage signal of the detection system is a linear function of the sample temperature, and the constant of proportionality is found in pretest experiments in which the temperature of the sample is changed with an auxiliary heating device.

However, during the plastic deformation of a metal, there are several changes besides those in the temperature, and these changes are manifested in the voltage records. It is well known that as an annealed metal is deformed the density of crystalline defects increases. The optical consequence is that the emissivity of the sample increases with strain. In addition, the surface topography changes with strain because of the inhomogeneous plastic flow which is characteristic of metals. This leads to several optical effects that must be taken into account for a proper calibration. Included in these changes is the change in degree by which the metal approximates a Lambert radiator. There is also a change in the radiation detectable from the surroundings that accompanies the topographical changes. This change occurs in part simply because the sample is a reflector so that changes in the orientation of surface elements can result in a change in the fraction of the energy detected from the mirrors of the detection system, the surroundings and the detector itself. Furthermore, some surface elements may become oriented relative to others in such a way that they reflect radiation from the sample, initially improperly directed for detection, toward the detector.

In the event that each of the detectable sources of energy is a continuous function of strain, it has been shown that the temperature change ΔT related to the voltage measurement ΔV is given by[13]

$$\Delta T = \frac{\Delta V - C\int_0^{ef} f(e)\, de}{(\partial V/\partial T)_{e_f}}, \qquad [6]$$

where $f(e) = \partial(E_i + E_1 + E_S + E_r)/\partial e$, E_i is the energy naturally emitted by the sample, E_1 is the difference in energy emitted from that of a Lambert radiator, E_S is the energy from the surroundings, E_r is the energy emitted from the sample that reaches the detector by reflecting off another part of the sample, e_f is the average strain over a gage length at least as large as the diameter of the field of view and C is a constant that is characteristic of the detection system and gives

the change in voltage per unit energy. Keeping track of strain on a smaller scale is not necessarily useful since the detector indiscriminantly adds the effects of all the energy it receives. If more than one strain level exists in the field of view, there can also be a continuum of thermal states. In the special case when plastic changes are adiabatic and occur on a smaller scale than the field of view, it might be possible to relate temperature changes with each of the microstrains. In this case, the fraction of the total radiation from each strain level must be known and taken into account.

The implication of Eq. [6] is that for special conditions one can determine the temperature of a deforming metal. There are other situations for which further precautions may be required. An example would be for the possible situation in which deformation induces a phase transformation that also depends on time.

At this point, it is worth elaborating further on the applicability of Eq. [6] in the light of real phenomena. The simplest situation arises when the inhomogeneities are on a fine scale with respect to the field of view and the heating appears uniform. Then, $f(e)$ and $(\partial V/\partial T)_e$ are readily determined since there is no noticeable variation with position on the sample. Temperature changes determined for these conditions are necessarily an average result.

The effect to be analyzed, however, was not in an average condition, but in the difference in thermal states of material bounding a plastic discontinuity. Without prior knowledge about the deformation, there is no way of knowing whether or not such a determination can be made. Accordingly, the IR detection system was used to establish some features of the deformation and the feasibility of measuring the temperature difference described. The measurements are described next along with a determination of $(\partial V/\partial T)_e$ after a fixed amount of deformation.

Characterization of Voltage Measurements

Each of the specimens used for calibration purposes, except one undeformed reference sample, was elongated quasistatically to a different strain, unloaded and equilibrated with room temperature for observations relative to $(\partial V/\partial e)_{T,x}$, $(\partial V/\partial x)_{T,e}$ and $(\partial V/\partial T)_{e,x}$. The final nominal strains were 4.86, 9.93, 14.39, 20.16, 26.69 and 28.23 pct. These strain measures were made over a 4 cm gage length, and are, therefore, an indication of the average strain only. The strain on a finer scale will be described later.

The average measured value of $\Delta V/\Delta T$ for the Cu in its initial state was 5.09 mV/°C. The deviation of the mean for these measurements was 0.19 mV/°C. After the Cu had been deformed 28 pct, this ratio was found to be 16.77 mV/°C. The deviation from the mean reflects scatter in the data that was primarily due to the fanning action of the chopper on the sample and variations with position in the optical properties of the chopper which noticeably affected the voltage signals.

Radiation measurements for the determination of changes in the signal voltage with position and strain for the Cu in the initial state and after elongation to each of the strains listed above were obtained by scanning the samples and chopping the radiation with the American Time Products tuning fork. A record representative of these measurements is shown in Fig. 12.

The records obtained for information about changes with position and strain were extremely informative. It is clear that at each strain level there were regions of the sample from which approximately constant amounts of radiation were detected. These regions were separated by boundaries that were thin compared with their width in the direction of scanning which was along the tensile axis (see Fig. 12). The subdivision of the samples into these regions was observable at all levels of plastic strain. Hence, it is concluded that these regions started to form simultaneously with yielding. The magnitudes of the voltage increments encountered as the samples were scanned from region to region increased with strain. The average of these incremental voltage changes is plotted in Fig. 13 vs average strain. While these voltage increments began at yield and became more prominent

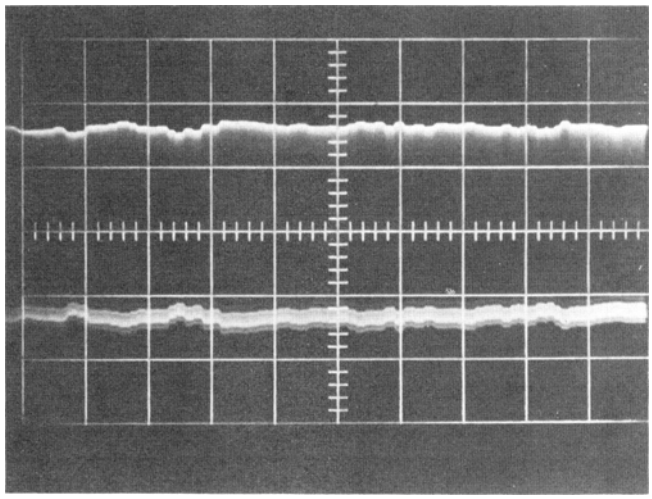

Fig. 12—Chopped signal from copper elongated 28.23 pct. 1 volt/cm vertical scale. Horizontal sweep corresponds to 1.27 cm on the copper surface parallel with the tensile axis.

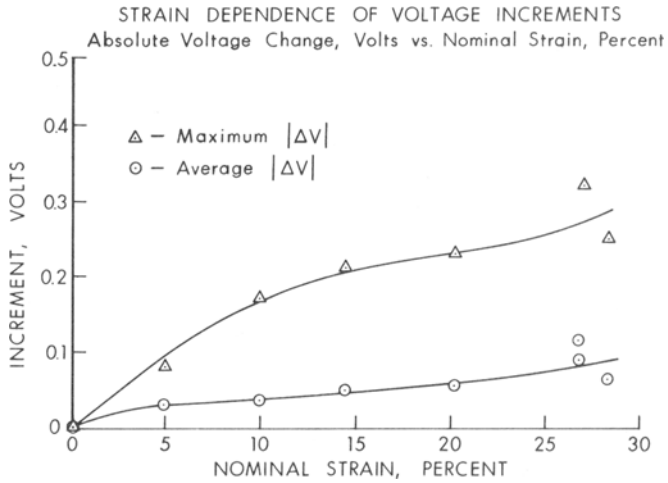

Fig. 13—Incremental voltage changes due to differences in the infrared radiation detected from adjacent regions in deformed copper.

with strain, the total number of regions per unit length along a sample changed only slightly with strain (see Fig. 14). The average number of regions over the length scanned, 1.27 cm, was approximately 63 so their average length was 0.02 cm. Let this length be $\bar{X}$.

The average detectable radiation from the copper increased with strain. This was measured as the change with strain in the peak-to-peak signal from the chopper and the sample, averaged over the total sample. This is a different measurement than the change in radiant energy from adjacent regions on a sample as described in the paragraph above. It was found that the average peak-to-peak voltage difference decreased with strain (see Fig. 15). Since the vanes of the American Time Products chopper were painted black, they emitted more energy than the copper when both were at the same temperature. Hence, the decrease in peak-to-peak voltage observed corresponds to an increased emittance of the copper with strain.

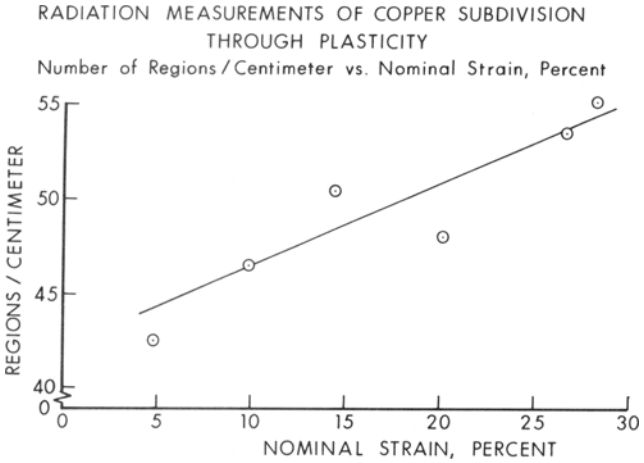

Fig. 14—The number of regions into which tensile specimens were subdivided by plastic deformation.

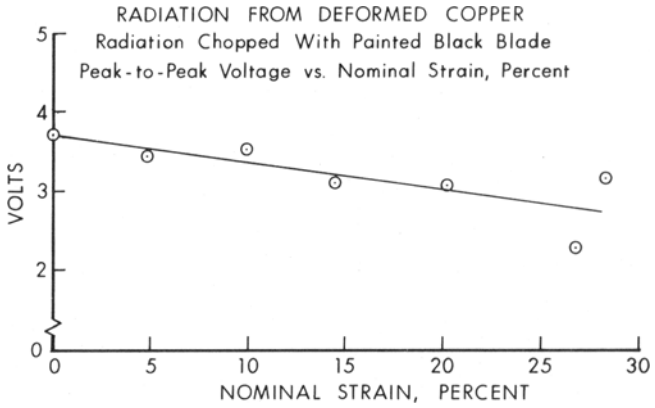

Fig. 15—Average change in radiation detectable from copper after deformation.

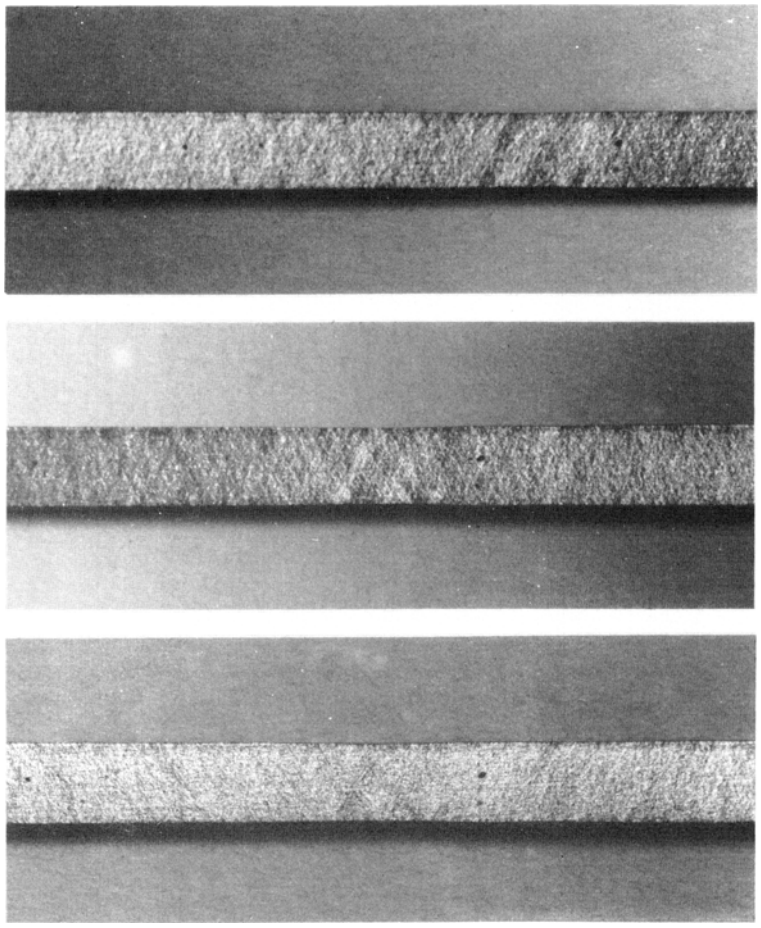

Fig. 16—Lüders bands in copper elongated 26.7 pct.

Scale of Deformation

The subdivision of the Cu revealed by the radiation records clearly indicates that 0.02 cm was an important dimension in the deformation. While the oscillographs very definitely documented the existence of the regions, there was nothing visible to the naked eye on the first samples observed that related to $\bar{X}$ in any way. At first, it was thought that the regions were the result of plastically induced topographical changes in the vicinity of grain boundaries. It had been demonstrated in preliminary tests that similar changes in detectable radiation did occur as grain boundaries were crossed in large-grained polycrystals. However, the average grain diameter of the surfaces monitored was only 0.00165 cm, which is much smaller than $\bar{X}$. This indicates that the regions in question depended on deformation that permeated several grains.

Visual and microscopic optical observations led to the identification of Lüders bands at large nominal strains. The bands occurred in several orientations and with irregular shapes. A photograph of clearly observable Lüders bands is shown in Fig. 16. This may be a new observation as no previous reports of Lüders band development in tensile specimens of copper are known to the authors. It is concluded that the regions revealed so distinctly with the IR detector were primarily Lüders bands. The implication is that the entire deformation involved the repetitive action of Lüders bands. Apparently, a finite development was required before they could be seen, which is why they were only visible at large strains. The simultaneous occurrence of yield and the formation of Lüders bands has been referenced repeatedly in the literature.[18] It is also usually accepted that the serrated stress-strain curve, or Portevin-Le Chatelier effect, is a consequence of yield type behavior.[19] Then, if yielding were through the formation of Lüders bands, it follows that, as strain proceeds, deformation might continue to be by Lüders bands. There are practically no reports in which it has been proposed that Lüders bands continue to function as such throughout the entire course of deformation, *i.e.*, to fracture. On the other hand, Phillips *et al.* have shown very elegantly that in aluminum-3 magnesium alloys Lüders bands continue to develop as long as the material is deformed.[9] The results reported in Figs. 12 through 14 are strong evidence that the progress of strain in copper can also be through the successive discontinuous functioning of Lüders bands.

It was convenient that, for the loading conditions and sample dimensions used, the widths of the Lüders bands were approximately equal to the field of view of the detection system. This condition left the possibility of measuring the maximum temperature difference between these bands and the adjacent parts of the sample with the IR detection system. Of course, sensible measurements could only be made if the heating within the Lüders bands were uniform.

It must be expected, however, that the heating within Lüders bands is not uniform since it arises from the micromechanisms of plastic flow, *i.e.*, dislocation motion and related annihilation processes. Accordingly, it would be incorrect to assume that the heating within a Lüders band could be represented by one temperature. Actually, there must be many thermal states within a deforming band rather than one.

On the other hand, it has been shown that the heating by the motion of individual dislocations, moved by stresses equal to or less than the ultimate tensile strength of the material, cause only small temperature changes.[20-22] These are on the order of a fraction of a degree. Furthermore, the maximum temperature change to be expected from dislocation annihilation is not more than approximately 3°C.[13] In addition, the heating by the motion and annihilation of individual dislocations must quench out quickly, and the slip within Lüders bands is distributed throughout the band. Under these conditions, it may be reasonable to assign an average temperature to a Lüders band and to view the thermal variations from dislocation motion and annihilation as temperature perturbations from the average. Then, if during deformation, average temperature changes of a degree or more are measured, they should be reasonably representative of the average temperature change within a Lüders band, and this was the point of view that was taken in treating the data of this report.

Data Interpretation

Eq. [6] is readily applicable to the determination of the temperature difference related to a plastic inhomogeneity 1) when there are distinct regions bounding a plastic transition that can be traversed by the detector and 2) when the regions involved are as large or larger than the field of view of the detector and 3) when each region is thermally uniform. The surface scans of the previously deformed samples indicated that to a first approximation these conditions did apply. Let the regions bounding the plastic transition be labeled A and B. Then, when the detector sensed radiation from Region A, the temperature change ΔT_A due to the strain $(e_f)_A$ from the initial state is given by Eq. [6]. A similar temperature change with strain, *i.e.*, ΔT_B, is recorded by the detector while viewing Region B. When the detector scans the sample during deformation and crosses a plastic transition zone, the temperature difference of the two regions is given by $\Delta T = \Delta T_A - \Delta T_B$. This assumes that the deformation that occurs while the transition zone is passed is negligible. Bursts of radiation that occur while the detector is essentially viewing a fixed area, as were apparently observed at the low strain levels, are not given by this difference. Those changes are given by a direct application of Eq. [6]. The thermal increments observed were treated as though they were revealed by the scanning of two regions facilitated by the stretching of the samples under the fixed focal point of the detector. However, it is noted that during a test, the signal from traversing a plastic transition zone could not be distinguished from the abrupt signal that would occur if a region suddenly deformed a great deal while in the field of view.

Proceeding as though the signals were primarily due to the passage of the field of view over a plastic transition zone and expanding the expression for ΔT with Eq. [6] gives the temperature difference as

$$\Delta T = \frac{(\Delta V)_A - (\Delta V)_B}{(\partial V/\partial T)_e} - \frac{C\left[\int_0^{(e_f)_A} f(e)\,de - \int_0^{(e_f)_B} f(e)\,de\right]}{(\partial V/\partial T)_e} \quad [7]$$

The first two terms in the numerator correspond to the voltage increments that were measured during a test, *i.e.*, $\Delta V_i = (\Delta V)_A - (\Delta V)_B$. The third term in the numerator is the correction for the nonthermal effects that have already been described, and its magnitude was measured as ΔV_p in the post test scans of the samples that were elongated to fixed strains. In those measurements, ΔV_p was calibrated with respect to the average strain of the sample, and the results are given in Fig. 13. An approximation was introduced into Eq. [7] by dividing the voltage changes of both regions by the value of $(\partial V/\partial T)_e$ that corresponded with the average sample strain. This was necessary since the exact localized strains of the sample were unknown. This approximation is not unreasonable since the value of $(\partial V/\partial T)_e$ was not strongly dependent on strain. Thus, to a first approximation the temperature differences due to the inhomogeneous nature of the deformation follow from Eq. [7] and are given by Eq. [1].

REFERENCES

1. J. Erdmann and J. Jahoda: Report D1-82-0384, Boeing Scientific Research Laboratories, Seattle, Washington, Oct., 1964.
2. A. Nadai and M. J. Manjoine: *J. Appl. Mech.*, 1941, vol. 8, pp. A-77-A91.
3. F. P. Bowden and P. H. Thomas: *Proc. Roy. Soc.*, 1954, vol. 233A, pp. 29-40.
4. J. W. Taylor: *J. Appl. Phys.*, 1963, vol. 34, pp. 2727-31.
5. N. C. Small: *Proc. of Infrared Session, Symposium,* Soc. for Nondestructive Testing, Raytheon Co., Wayland, Massachusetts, 1966.
6. P. J. King, D. F. Cotgrove, and P. M. B. Slate: *Behavior of Dense Media Under High Dynamic Pressure,* p. 513, Gordon and Breach, New York, 1968.
7. Paul A. Urtiew and Richard Grover: *Temperature, Its Measurement and Control in Science and Industry,* vol. 4, part I, H. H. Plumb, ed., p. 677, Instrument Society of America, Pittsburgh, 1972.
8. R. K. Linde and D. G. Doran: *Nature,* 1966, vol. 212, pp. 27-29.
9. V. A. Phillips, A. J. Swain, and R. Eborall: *J. Inst. Metals,* 1952, vol. 81, pp. 625-47.
10. C. E. Mobley, Jr.: Ph.D. Thesis, Johns Hopkins University, 1968.
11. J. F. Bell: *The Physics of Large Deformation of Crystalline Solids,* pp. 33 and 77, Springer-Verlag, New York, 1968.
12. T. N. Rhodin, Jr.: *J. Amer. Chem. Soc.*, 1950, vol. 72, p. 5102.
13. G. L. Moss: Ph.D. Thesis, Johns Hopkins University, 1972.
14. Lord Kelvin: *Trans. Roy. Soc. Edinburgh,* 1851; *Mathematical and Physical Papers,* vol. III, pp. 236-38, C. J. Clay and Sons, Cambridge University Press Warehouse, London, 1890.
15. R. M. Fisher and J. S. Lally: *Can. J. Phys.*, 1967, vol. 45, pp. 1147-59.
16. J. F. Bell: *The Physics of Large Deformation of Crystalline Solids,* pp. 205-12, Springer-Verlag, New York, 1968.
17. W. N. Sharpe, Jr.: *J. Mech. Phys. Solids,* 1966, vol. 14, p. 187.
18. A. Nadai: *Theory of Flow and Fracture of Solids,* vol. 1, pp. 275-96, McGraw-Hill, New York, 1950.
19. A. W. McReynolds: *Trans. AIME,* 1949, vol. 185, pp. 32-45. (*Metals Technology,* January 1949, pp. 32-45.)
20. F. Seitz: *Advan. Phys.*, 1952, vol. 1, pp. 43-90.
21. J. D. Eshelby and P. L. Pratt: *Acta Met.*, 1956, vol. 4, pp. 560-62.
22. A. M. Fruedenthal and J. H. Weiner: *J. Appl. Phys.*, 1956, vol. 27, pp. 44-50.